

Quantum phases of a frustrated spin-1 system: The 5/7 skewed ladder

Sambunath Das^{1,*}, Dayasindhu Dey^{1,†}, Manoranjan Kumar^{2,‡} and S. Ramasesha^{1,§}

¹*Solid State and Structural Chemistry Unit, Indian Institute of Science, Bangalore 560012, India*

²*S. N. Bose National Centre for Basic Sciences, Block JD, Sector III, Salt Lake, Kolkata 700106, India*



(Received 14 December 2020; revised 20 August 2021; accepted 15 September 2021; published 27 September 2021)

The quantum phases in a spin-1 skewed ladder system formed by alternately fusing five- and seven-membered rings are studied numerically using the exact diagonalization technique up to 16 spins and using the density matrix renormalization group method for larger system sizes. The ladder has a fixed isotropic antiferromagnetic (AF) exchange interaction ($J_2 = 1$) between the nearest-neighbor spins along the legs and a varying isotropic AF exchange interaction (J_1) along the rungs. As a function of J_1 , the system shows many interesting ground states (gs) which vary from different types of nonmagnetic and ferrimagnetic gs. The study of various gs properties such as spin gap, spin-spin correlations, spin density, and bond order reveal that the system has four distinct phases, namely, the AF phase at small J_1 ; the ferrimagnetic phase with gs spin $S_G = n$ for $1.44 < J_1 < 4.74$ and with $S_G = 2n$ for $J_1 > 5.63$, where n is the number of unit cells; and a reentrant nonmagnetic phase at $4.74 < J_1 < 5.44$. The system also shows the presence of spin current at specific J_1 values due to simultaneous breaking of both reflection and spin parity symmetries.

DOI: [10.1103/PhysRevB.104.125138](https://doi.org/10.1103/PhysRevB.104.125138)

I. INTRODUCTION

In low-dimensional magnetic systems, confinement leads to strong quantum fluctuations, and these systems can show many exotic phases in the presence of frustration induced by the topology of exchange interactions [1–21]. Even in a one-dimensional (1D) spin system, with only a nearest-neighbor Heisenberg antiferromagnetic (HAF) exchange interaction, the ground state (gs) can be gapped or gapless for integer or half odd-integer spins, respectively, as pointed out in a seminal paper by Haldane [22]. The gs of the HAF integer spin chain can be represented as a valance bond solid (VBS) [23–25], and in 1987 Affleck, Kennedy, Lieb, and Tasaki (AKLT) showed that perfect VBS state may exist on various geometries with specific spins [23,24]. The AKLT state still continues to inspire physicists for various reasons; for example, the AKLT state has led to many recent developments such as the matrix product states technique [26–28], which is a form of the density matrix renormalization group (DMRG) method [29–32]; the tensor network method [33]; and the projected entangled pair states ansatz [27,28]. AKLT states can also be represented as cluster states which can be used in measurement-based quantum computation [34,35], and recently these states have been explored in a spin-3/2 on a hexagonal lattice [36,37].

The HAF spin-1 chain exhibits a topological phase, spin-1/2 edge modes, and the gs is fourfold degenerate in the thermodynamic limit. The correlation length in the gs of spin-1 is 6.05 lattice units and the eigenvalue spectrum has large spin gaps [38,39]. The gs can be represented as a

VBS, which belongs to the same universality class of AKLT states [23,24]. The two leg HAF spin-1 ladder shows interesting properties like plaquette-singlet solid state, where two spin-1/2 singlet dimers are sitting at each rung and there is no overlap between the VBS states in the large rung exchange limit [40]. The AKLT state in the system breaks down for any finite value of rung exchange interaction [40]. The spin-1 zigzag ladder shows a transition from a Haldane phase to a double Haldane phase [41,42]. In fact, the zigzag ladder can be mapped into a chain system with nearest-neighbor and next-nearest-neighbor exchange interactions, and the gs of the frustrated systems is a singlet. In this work, we explore the magnetic phases of a spin-1 system on a 5/7-skewed ladder system; it has been demonstrated that a spin-1/2 system on this lattice shows many exotic phases [43].

The 5/7-skewed ladder is inspired by fused Azulene, a ladderlike structure made up of 5- and 7-membered carbon rings alternately fused on a chain, studied by Thomas *et al.* in which they showed that the gs is ferrimagnetic [44]. These structures can be mapped to a zigzaglike ladder structure with some missing bonds [43,44]. The HAF spin-1/2 system on various lattices such as the 5/7, 3/4, 3/5, and 5/5 is studied and it was shown that the gs of these systems exhibits many interesting magnetic and nonmagnetic gs in their quantum phase diagrams with strength of the rung exchange interaction as a phase parameter [43]. In the large rung exchange limit, the gs wave function of a 5/7 skewed ladder can be represented as a product of rung singlet dimers and two ferromagnetically interacting spins per unit cell [45]. In various parameter regimes this system shows dimer, spiral, and chiral vector phases [43]. In the presence of an axial magnetic field, the HAF spin-1/2 system on the 5/7 skewed ladder exhibits four magnetization plateau phases [45].

* sambunath.das46@gmail.com

† dayasindhu.dey@gmail.com

‡ manoranjan.kumar@bose.res.in

§ ramasesha@iisc.ac.in

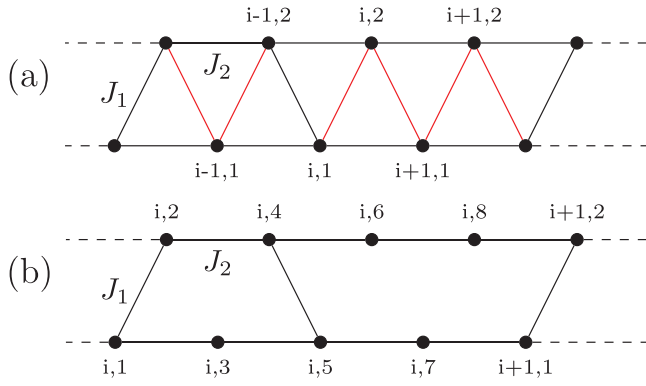


FIG. 1. Schematic diagram of (a) a zigzag ladder. The nearest neighbor or rung interaction is J_1 and the next-nearest neighbor (along the leg) interaction is J_2 . (b) The 5/7 skewed ladder: Some rung bonds shown in red of the zigzag ladder are periodically removed to give a 5/7 skewed ladder. Here “ i ” is the index of the unit cell and the numerals 1, 2, ... are numbering of the spins within the unit cell. There are 2 spins per unit cell in the zigzag ladder while there are 8 spins per unit cell in the 5/7 ladder. The sites on the top leg are even numbered and on the bottom leg are odd numbered.

The structure of zigzag and a 5/7 skewed ladder are shown in Figs. 1(a) and 1(b) and by periodically removing some of the rung bonds, shown in red, from Fig. 1(a) to give 5/7 skewed ladder in Fig. 1(b). In this paper, we are interested in the gs phases of a spin-1 5/7 skewed ladder as a function of the ratio of rung-to-leg exchanges J_1 and J_2 , respectively. We show that this system is highly frustrated, and in the small rung interaction limit, $J_1/J_2 < 1.06$, singlet dimers along the rung are weak and correlations along the leg remain short ranged, whereas for $J_1/J_2 > 1.44$, the gs is magnetic and each unit cell contributes spin-1 to the gs spin S_G , and spin densities are distributed over the whole unit cell, with spin density at sites 3 and 7 being large. For $4.74 < J_1/J_2 < 5.44$ the system is nonmagnetic but for $J_1 > 5.63$ gs of the system is magnetic with each unit cell contributing spin 2 to S_G with prominent rung dimers and site spin densities.

This paper is divided into four sections. In Section II we discuss the model Hamiltonian and the numerical methods. The results are presented and discussed in Section III under four subsections. Section IV provides a summary of results and conclusions.

II. MODEL AND METHOD

The site numbering used in this paper for the 5/7 skewed ladder is shown in Fig. 1(b). All nonzero exchange interactions between spins are antiferromagnetic (AF). The sites are numbered such that odd numbered sites are on the bottom leg and even numbered sites are on the top leg. Thus the rung bonds are the nearest-neighbor exchanges J_1 and the bonds on the legs are the next-nearest-neighbor exchanges J_2 . The exchange J_2 is set to 1 and it defines the energy scale. The model Hamiltonian of the 5/7 skewed ladder can be

written as

$$H_{5/7} = J_1 \sum_i (\vec{S}_{i,1} \cdot \vec{S}_{i,2} + \vec{S}_{i,4} \cdot \vec{S}_{i,5}) + J_2 \sum_i \left(\vec{S}_{i,7} \cdot \vec{S}_{i+1,1} + \vec{S}_{i,8} \cdot \vec{S}_{i+1,2} + \sum_{k=1}^6 \vec{S}_{i,k} \cdot \vec{S}_{i,k+2} \right), \quad (1)$$

where i labels the unit cell and k are the spins within the unit cell (Fig. 1). The first term denotes the rung exchange terms, and the second term denotes the exchange interactions along the legs.

We use the exact diagonalization technique for finite ladders with up to 16 spins and impose periodic boundary condition (PBC). There are mirror planes perpendicular to the ladder, for example, the plane perpendicular to the ladder and passing through site 3 and the perpendicular bisector of sites 2 and 4, as well as the one passing through site 7 and the perpendicular bisector of sites 6 and 8, again perpendicular to the ladder. An extra rung is needed when the open boundary condition (OBC) is used. For larger system sizes we use the DMRG method [29–32] to handle the large degrees of freedom in the many-body Hamiltonian. We retain up to 500 block states ($m = 500$), which are the eigenvectors of the block density matrix with dominant eigenvalues. The chosen value of “ m ” keeps the truncation error to less than $\sim 10^{-10}$. We also carry out 6–10 finite sweeps for improved convergence. The details of building the 5/7 ladder for the DMRG method is the same as in Ref. [43]. The largest system size studied is a system with 130 sites or 16 unit cells with OBC. The DMRG calculations are carried out for different S^z values of ladders. The gs spin is $S_G = l$, for l that satisfies $\Gamma_l = 0$ and $\Gamma_{l+1} > 0$, where Γ_l is given by

$$\Gamma_l = E_0(S^z = l) - E_0(S^z = 0), \quad (2)$$

with E_0 being the lowest energy state in the chosen S^z sector. The correlation function and bond orders are computed in the gs, with $S^z = S$.

III. RESULTS AND DISCUSSIONS

In the gs, the spin-1 5/7 skewed ladder, like the spin-1/2 system, also shows many exotic phases like the bond order wave (BOW) phase, chiral points in parameter space of the Hamiltonian and nonmagnetic to magnetic phase transition on tuning the value of J_1 . However, there are significant differences from the spin-1/2 system. To analyze the magnetic transitions in the quantum phase diagram, various quantities are analyzed as a function of J_1/J_2 which is the only variable model parameter in this system and J_2 is set to 1. Besides the spin gaps Γ_l , we have the computed correlation function $C(r) = \langle \vec{S}_i \cdot \vec{S}_{i+r} \rangle$ to study the behavior of the spins in the system. The bond order between bonded neighbors $-\langle \vec{S}_i \cdot \vec{S}_{i'} \rangle$, where sites i and i' are bonded neighbors, and spin-density $\langle S_i^z \rangle$ within a unit cell are also calculated and compared with the results for a 1D spin-1 chain where appropriate.

A. Nature of gs

The spin in the gs, S_G , of the skewed 5/7 ladder systems is obtained from the magnetic gaps Γ_l defined in Eq. (2). In

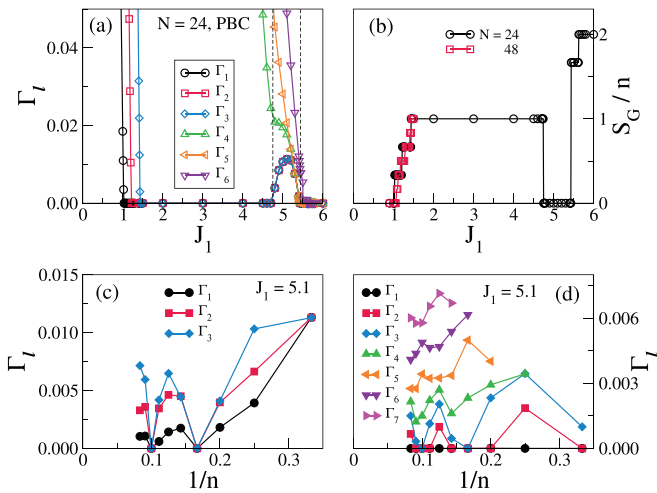


FIG. 2. (a) The lowest excitation gaps Γ_l for different $S^z = l$ manifolds are shown as functions of J_1 . For $J_1 < 1.06$, Γ_1 is nonzero, whereas for $1.06 < J_1 < 4.74$, Γ_l is zero for $l \leq S$ where S is the total spin of the gs. The system exhibits reentrant nonmagnetic phase for $4.74 < J_1 < 5.44$ where Γ_1 is nonzero. For $1.44 < J_1 < 4.74$ $S_G \sim n$ and for $J_1 > 5.63$ $S_G \sim 2n$. (b) The variation of the gs spin per unit cell S_G/n with J_1 for system sizes of 48 ($n = 6$) spins in regions I and II and of 24 ($n = 3$) spins in all the regions. (c) The lowest excitation gaps Γ_1 , Γ_2 , and Γ_3 with the inverse of the number of unit cells of a $5/7$ with PBC are shown for $J_1 = 5.1$. (d) The lowest excitation gaps Γ_1 to Γ_7 with the inverse of the number of unit cells of a $5/7$ with OBC are shown for $J_1 = 5.1$.

Fig. 2(a), we plot the gaps Γ_l for different values of “ l ” as a function of J_1 for a system with 24 spins corresponding to 3 unit cells ($n = 3$) under PBC. The plot shows that there are four distinct regions: In region I with $0 < J_1 < 1.06$, the gs is a singlet and is nonmagnetic; in region II, $1.06 < J_1 < 4.74$, S_G is less than or equal to the number of unit cells in the systems; consequently, each unit cell contributes at most spin-1 to S_G and for $1.44 < J_1 < 4.74$, the spin S_G saturates to the number of unit cells. We calculate S_G/n as a function of J_1 for systems with $N = 24$ and $N = 48$ spins to investigate if the transition to $S_G = n$ is smooth or abrupt. We find that S_G/n shows a gradual increase in the region $1.06 < J_1 < 1.44$ for the larger system, shown in Fig. 2(b). The weak finite size effect in S_G/n can be attributed to the short spin-spin correlation lengths. As shown in Fig. 2(b), the increase in S_G/n is continuous between regions I and II. In region III, $4.74 < J_1 < 5.44$, the gs becomes nonmagnetic for the 24 spin system. The spin-spin correlation function reveals that in this region, the “free” spins in each unit cell align ferromagnetically while the alignment of the spins across unit cells is AF, with large periodicity. The transition from region II to region III is abrupt for $N = 24$ spins and we had convergence difficulties even for the $N = 48$ spins and hence cannot comment on the effect of system size.

We investigated the spin gaps at $J_1 = 5.1$ (where there is a peak in the Γ_l values for the $N = 24$ spin system) as a function of system size from $N = 24$ to $N = 96$ spins, retaining 2400 block states in the finite DMRG calculations for both PBC and OBC. We find that for this J_1 value, the gaps Γ_1 to Γ_n exhibit nonlinear variation with system size as shown in Figs. 2(c)

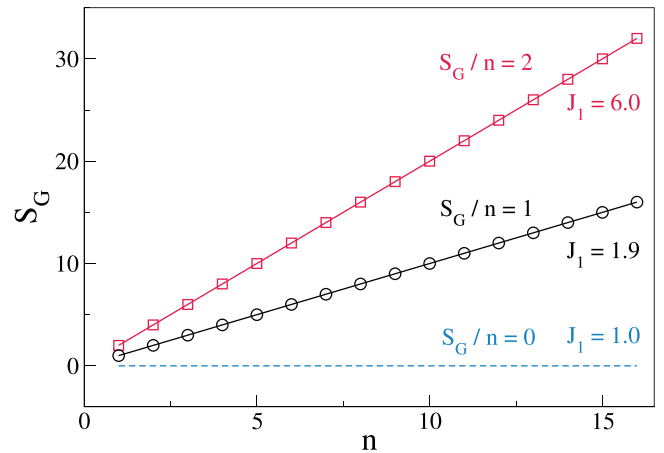


FIG. 3. The variation of the gs spin S_G with the number of unit cells n shown for $J_1 = 1.0, 1.9$, and 6.0 .

and 2(d) for PBC and OBC, respectively. The convergence for higher values of l in Γ_l for PBC is poor and hence is not shown in Fig. 2(c). We find that for some system sizes (number of unit cells n) the excitation gaps Γ_1 , Γ_2 , and Γ_3 vanish for both PBC and OBC. We surmise that the vanishing of the gaps is because for “ n ,” the number of unit cells in the system is an integral multiple of the periodicity of the spin-spin correlations. In region IV, the spin of the gs is $2n$ and indicates that all the free spins are ferromagnetically aligned. The transition from region III to region IV was followed for the 24 spin system under PBC by varying J_1 in small increments. We find a step in the gs spin at an intermediate value $1 < S_G/n < 2$ with a step width of 0.18 in J_1 , but this region could not be studied for larger system sizes due to convergence difficulties. In region IV, with $J_1 > 5.63$, S_G corresponds to twice the number of unit cells. We summarize the behavior of the gs in different regions in Fig 3.

B. Spin correlations

To understand the spin structure in different regions of the parameter space, we have studied the spin-spin correlations of the total spin $C(r) = \langle \vec{S}_k \cdot \vec{S}_{k+r} \rangle$, where k is the reference site of spins in the middle of the system. The z component of the spin correlations, $C^{zz}(r) = \langle S_k^z S_{k+r}^z \rangle - \langle S_k^z \rangle \langle S_{k+r}^z \rangle$, shows behavior similar to the total spin correlation. The total spin correlations are shown for a system of 98 spins, which correspond to 12 unit cells for OBC. These are calculated in the gs with $S^z = S_G$. There are three different spin correlations that we have computed. They correspond to the correlation between spins on the lower leg $C_1(49, 49 + 2r)$, $C_2(50, 50 + 2r)$ between spins on the upper leg and $C_3(51, 51 + 4r)$ between free spins which reside on the lower leg. The reference site for the correlations is from the middle unit cell which for C_1 is site 49, for C_2 is site 50, and for C_3 is site 51. For convenience, we classify the spins on the lower leg as of two types, type 1 “bound” spins, which are bound to three nearest-neighbor spins, and type 2 as free spins, which are the middle sites in the five- and seven-membered rings.

In Fig. 4, we show the spin correlations in the four different regions of the parameter space. The correlations $C_1(r)$

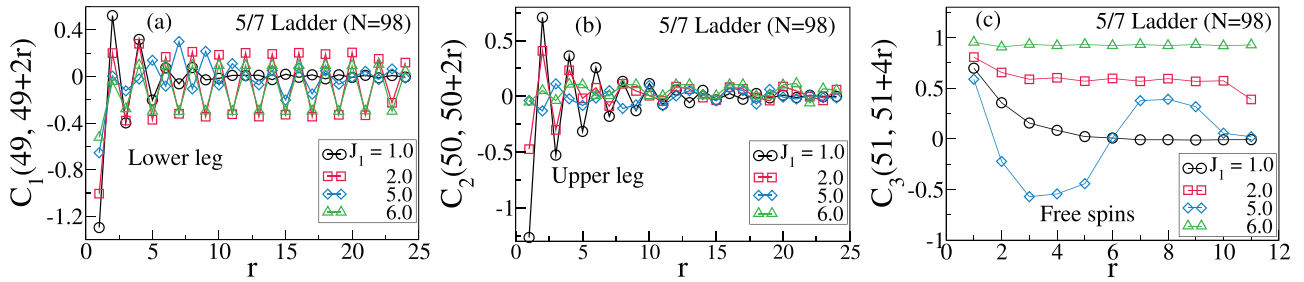


FIG. 4. The spin-spin correlations between (a) spins in the lower leg, (b) spins in the upper leg, and (c) free spins at sites 3, 7, 11, etc. for a 5/7 ladder with $N = 98$ spins with OBC. Four J_1 values are chosen to represent different regions of the phase diagram. $J_1 = 1.0$ for the nonmagnetic phase, $J_1 = 2.0$ for the $S_G = n$ phase, $J_1 = 5.0$ for the reentrant phase, and $J_1 = 6.0$ for the $S_G = 2n$ phase.

shown in Fig. 4(a) correspond to spins in the lower leg. The correlations are given from site 49 which is in the middle of the system. For $J_1 = 0$, we have the correlation length of the Haldane system. We also find that as J_1 is increased, the correlation length gradually decreases to ~ 2.2 for $J_1 = 1.0$. In the transition region between I and II, the correlations fluctuate rapidly and we cannot extract a correlation length. We note that for $J_1 = 1.0$, the system has a singlet gs. The correlations fall off rapidly and the correlation length ξ is ~ 2.2 sites of the specified kind. In the spin-1 AF chain, the correlation length is longer by almost a factor of three and is approximately six sites. The shorter correlation length can perhaps be attributed to the frustration in exchange interactions in the rings. For $J_1 = 2.0$ and 6.0 , the system is in a magnetic state, and $C_1(r)$ decays very slowly and is AF in nature. In the reentrant phase, the system goes to a nonmagnetic state, and the spin correlations between the spins on the lower leg have long wavelength spin oscillations whose amplitude shows an exponential decay and corresponds to a noncollinear spin arrangement. From the spin correlations, it appears that the magnetic unit cell is tripled in this region. In Fig. 4(b), $C_2(r)$ in the upper leg is shown for the four phases, with the reference spin being the 50th spin in the system. $C_2(r)$ for both $J_1 = 1$ and 2 is AF and exponentially decaying with correlation length, $\xi \approx 3$. For $J_1 = 5$ and 6 , $C_2(r)$ is vanishingly small, the magnitude is less than ≈ 0.05 , even for nearest neighbor pair, and shows long wavelength behavior. However, the amplitude of this wave is too small to definitively conclude this oscillatory behavior. The small correlation in the upper leg at high J_1 is due to the strong dimer formation along the rungs and between the $(i, 6)$ and $(i, 8)$ sites. The correlations between free spins $C_3(r)$ show a rapid decay in the nonmagnetic state at $J_1 = 1$, while those for $J_1 = 2$ and $J_1 = 6$, the correlations are ferromagnetic. For the $J_1 = 6$, the spins at these sites have almost completely aligned ferromagnetically, while for $J_1 = 2$, the alignment is partially ferromagnetic. This reflects in the net spin of the gs which is $2n$ for the $J_1 = 6$ case and n for the $J_1 = 2$ case. In the reentrant phase, the free spins in each unit cell are aligned ferromagnetically, while the alignment of these spins across unit cells is AF, with large periodicity.

In summary, all the nearest-neighbor spin correlations are always AF in the nonmagnetic gs for J_1 in regime I, and the correlation lengths are much shorter than the Haldane chain. For J_1 values in regime-II where $S_G \sim n$, the correlations in the lower leg are AF and very long ranged, while those in the

upper leg are AF and fall off rapidly. The free spin correlations are ferromagnetic with an amplitude of about 0.6 and show very slow decay. When the J_1 value is in the reentrant regime III, the lower leg spin correlations show formation of wave packets over approximately three unit cells. The free spin correlations show a long wavelength oscillatory behavior with about five unit cell wavelength, which corresponds to a long period Néel arrangement of free spins. While in the classical, frustrated $J_1 - J_2$ model, the pitch angle is dependent on J_1/J_2 , in the skewed ladder, we have not been able to obtain a similar relationship. Besides, it is unlikely that a classical model will exhibit a reentrant phase. In regime IV, the bound spins on the lower leg are antiferromagnetically aligned and the correlations fall off very slowly with distance. The correlations between spins on the upper leg show weak long period Néel structure. The free spins are aligned ferromagnetically with very long correlation length.

C. Spin densities and bond order

The correlation lengths in the system are short, often less than the distance to a third equivalent nearest neighbor. Hence, we can get qualitatively correct behavior of the system in the thermodynamic limit from high accuracy DMRG studies on a system with three unit cells. We have carried out studies on a 48 site spin-1 system, with PBC corresponding to six unit cells ($n = 6$). We have retained 2400 block states for high accuracy in our DMRG computations. We have computed the spin densities in the gs for $S^z = S_G$ and the bond orders of all the nearest-neighbor bonds. The system has reflection symmetry and hence there are five unique bonds and five unique sites. The spin densities are computed as the expectation value of $\langle \psi_{gs} | S_i^z | \psi_{gs} \rangle$. They are uniformly zero in the singlet gs. The bond orders are computed as $b_{i,j} = -\langle \psi_{gs} | S_i \cdot S_j | \psi_{gs} \rangle$, where i and j are nearest-neighbor bonds. When the gs of the system is a singlet (region I), from the bond orders (Fig. 5) we can describe the system as weakly coupled spin-1 HAF chains. The upper leg has a BOW with a periodicity of four bonds, while the lower leg has a BOW with a periodicity of two bonds. The rung bonds are weak and the leg bond orders vary between 1.285 and 1.370. For comparison, in the spin-1 HAF, all the bond orders are uniform and have a value of 1.40. In region II, where $S_G = n$, the upper leg bond between the sites in the pentagon becomes weak, the rung bonds become strong, and the bonds in the lower leg

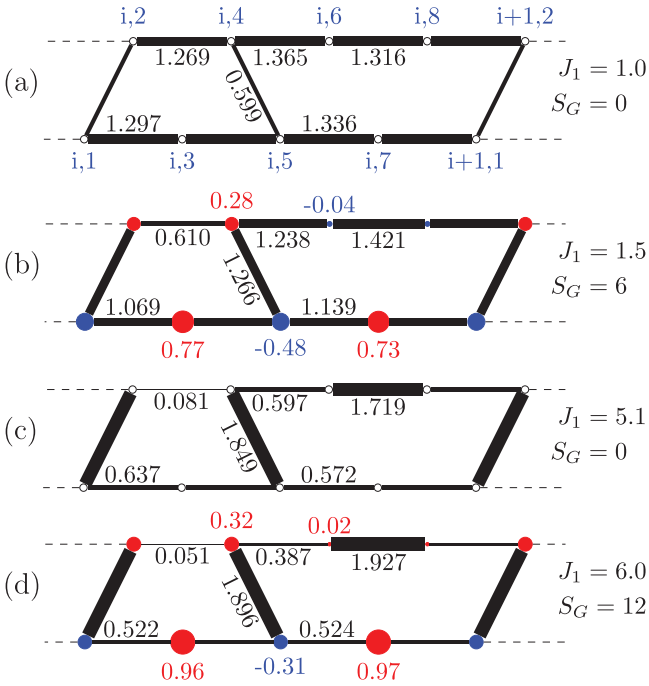


FIG. 5. Bond orders for 5/7 skewed ladder with $N = 48$ spins and PBC in the four different regions: (a) Nonmagnetic at $J_1 = 1.0$, (b) $S_G = n$ at $J_1 = 1.5$, (c) reentrant nonmagnetic at $J_1 = 5.1$, and (d) $S_G = 2n$ at $J_1 = 6.0$. The numbers adjacent to the bonds are the bond orders. The width of the bonds is proportional to the magnitude of the bond order. The site numbering is given in (a), the zero spin density is represented by open circles in (a) and (c), the spin density in (b) and (d) is proportional to the area of the filled circles. Red circles represent positive spin densities and blue circles represent negative spin densities.

also become slightly weak. Besides, the bond on the upper leg between the sites, which entirely belongs to the seven-membered ring, also becomes strong. The rung bonds become much stronger while the ladder bonds become weaker. The spin densities at the free spin sites are nearly equal and there is a net negative spin density on the rung bonds with the spin density of the sites on the lower leg being large negative. The “bonded” spin sites on the seven-membered ring on the upper leg acquire small negative spin densities. In region IV, where the $S_G = 2n$, the rung bonds and the bond in the upper leg of the seven-membered ring almost form singlets, with a bond order close to 2.0. All other bonds are very weak. The spin densities of the sites in the seven-membered ring which form the singlet are very nearly zero, while the rung bonds are qualitatively different with large negative (on the lower leg) and positive (on the upper leg) spin densities. The free spins are almost completely polarized and have spin densities that are very nearly unity.

D. Vector chirality

Broken symmetry states give rise to different quantum phases whose properties depend on the type of symmetry that is broken in the system. In general, broken spatial inversion/reflection symmetry gives rise to the BOW phase, whereas broken spin inversion symmetry gives rise to spin-

density wave (SDW). If both the spatial and spin inversion symmetries in the system are broken, then the vector chiral phase arises and it leads to a spontaneous spin current in the system. For these symmetries to break simultaneously, the lowest energy states in the two subspaces that the symmetry element divides the appropriate Hilbert space should be degenerate. In this case, any linear combination of the two low-lying states in the two subspaces, which are even (odd) under both reflection and spin inversion, will be degenerate resulting in symmetry breaking. The symmetry group of the 5/7 skewed ladder system consists of four elements: E , P , σ , and σP , where E is identity, σ is the reflection symmetry, and P is the spin inversion symmetry, and all these elements commute with each other leading to an Abelian group. The four irreducible representations correspond to A^+ , A^- , B^+ , and B^- . A (B) corresponds to even (odd) under σ while “+” (“-”) corresponds to even (odd) under P . A BOW transition requires a degeneracy between the lowest states in A^+ and B^+ (or A^- and B^-) subspaces. Similarly, an SDW transition requires a degeneracy of the lowest energy states in A^+ and A^- (or B^+ and B^-) subspaces. For a vector chiral transition, the lowest energy states in A^+ and B^- (or A^- and B^+) subspaces must be degenerate. Since the spin inversion symmetry, P divides the $S^z = 0$ subspace into even and odd total spin (S) sectors, the lowest energy states of the odd and even subspaces under P should be degenerate to break the spin inversion symmetry. To determine the degeneracy of the lowest energy state in the odd and even subspaces under spin inversion symmetry, instead of employing “ P ” to divide the Hilbert space with $S^z = 0$ into even and odd total spin subspaces, we use the following argument. Whenever there is a degeneracy of the lowest energy states with odd and even total spin sectors, then the spin inversion symmetry is broken. We recognize the degeneracy of the gs when two states in the $S^z = 0$ sector are degenerate. In this case, we compute the energies of the lowest states in the higher S^z sectors. The spin of the degenerate spin states is determined by following the degeneracies of the states in these sectors.

We calculate the energy gap Γ_σ as the modulus of the difference in energy between the lowest energy states in the A and B subspaces,

$$\Gamma_\sigma = |E_0(\sigma = -1) - E_0(\sigma = +1)|, \quad (3)$$

where $E_0(\sigma = +1)$ and $E_0(\sigma = -1)$ are the lowest energies in the even and odd subspaces under σ . In Fig. 6, Γ_σ is shown as a function of J_1 for a system size $N = 16$ with PBC. We see that it vanishes at four values of J_1 , namely, $J_1 = 1.07$, $J_1 = 1.408$, $J_1 = 4.601$, and $J_1 = 5.550$. At these values of J_1 , we compute Γ_l and find the two degenerate gs have spins $S = 0$ and 1, $S = 1$ and 2, $S = 2$ and 3, and $S = 3$ and 4, respectively, at $J_1 = 1.07$, 1.408, 4.6, and 5.550. In Table I we show the lowest energy states in different S^z sectors at the four points at which Γ_σ vanishes. The degeneracy under reflection and spin inversion at a given J_1 implies a vector chiral state and nonzero spin currents for these J_1 values.

Usually, in all known systems, the chiral phase emerges either due to exchange anisotropy or due to an external magnetic field on a ferrimagnetic gs. However, in our system, due to the peculiar nature of the frustrated exchange interactions, accidental degeneracy occurs between the lowest

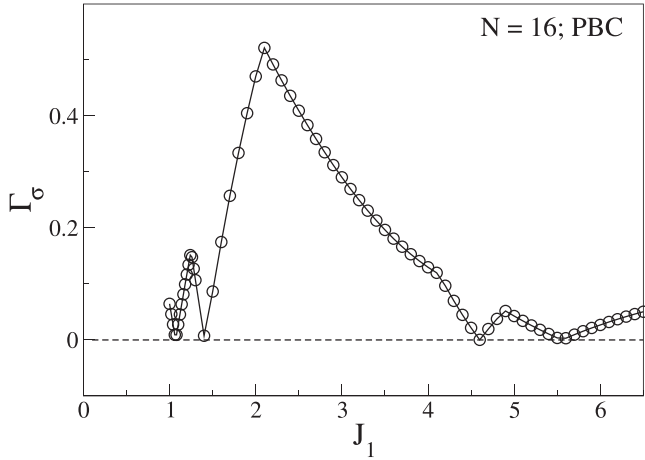


FIG. 6. The energy gap Γ_σ [see Eq. (3)] between two lowest energy levels belonging to different reflection symmetry subspaces. Γ_σ vanishes at $J_1 = 1.07, 1.408, 4.601,$ and 5.55 indicating degeneracies at these J_1 values.

energy states in the A^+ and B^- symmetries. In the basis of these degenerate states, the spin chirality operator has nonzero eigenvalues. This leads to nonzero spin current in a well-defined S_z state, but the total spin is no longer conserved in the eigenstate. This implies spontaneous symmetry breaking, i.e., the eigenstate does not exhibit the full symmetry of the Hamiltonian.

The magnitude of the z component of the spin current, $\kappa_z(j, k)$, is given by the eigenvalues of the matrix of the spin current operator for the $j - k$ bond, viz., $(\vec{S}_j \times \vec{S}_k)_z$ in the $|\psi_G(\pm)\rangle$ basis. The matrix, in this basis, is given by,

$$\begin{pmatrix} \langle \psi(+) | \hat{\kappa}_z | \psi(+) \rangle & \langle \psi(+) | \hat{\kappa}_z | \psi(-) \rangle \\ \langle \psi(-) | \hat{\kappa}_z | \psi(+) \rangle & \langle \psi(-) | \hat{\kappa}_z | \psi(-) \rangle \end{pmatrix},$$

where the function $|\psi_G(+)\rangle$ is the lowest energy state in the even subspace for reflection and even subspace for spin inversion, similarly, $|\psi_G(-)\rangle$ is in the odd subspace under both symmetries. The matrix elements of the spin current operator can be evaluated easily by using the operator identity

$$\kappa_z(j, k) = -i(\vec{S}_j \times \vec{S}_k)_z = \frac{1}{2}(S_j^+ S_k^- - S_j^- S_k^+). \quad (4)$$

The diagonal matrix element in the 2×2 matrix is zero, and the eigenvalues of the spin current are given by $\pm \frac{1}{2} |\langle \psi_G(\pm) | (S_j^+ S_k^- - S_j^- S_k^+) | \psi_G(\pm) \rangle|$.

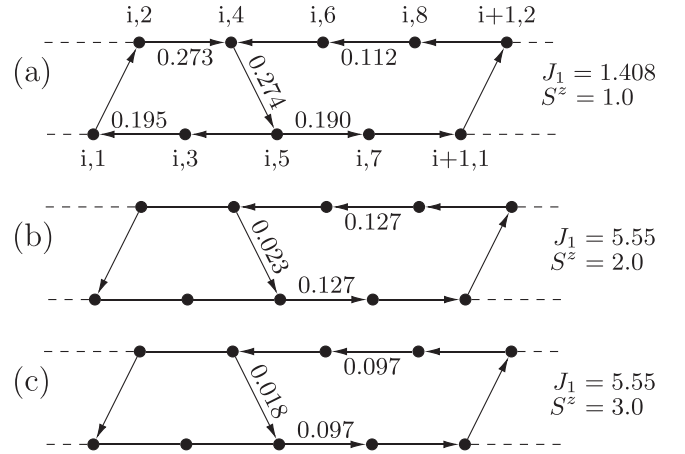


FIG. 7. Spin currents $\kappa_z(j, k)$ of a $5/7$ skewed ladder of $N = 16$ spins [see Eq. (4)] for (a) $J_1 = 1.408$ in the $S^z = 1$ sector, (b) $J_1 = 5.55$ in the $S^z = 2$ sector, and (c) $J_1 = 5.55$ in the $S^z = 3$ sector. Arrows indicate the direction of the current, and the magnitude of the currents is given adjacent to the arrows. No arrowhead for a bond means the spin current is zero along that bond.

In Fig. 7, we show the spin currents for $J_1 = 1.408$ and 5.550 for different degenerate S^z values. Spin currents for all J_1 values, at which $\Gamma_\sigma = 0$ and there is a degeneracy between states of odd and even total spin, are shown in Table II for different S^z values. We find that the spin currents are large for $J_1 = 1.408$ compared with $J_1 = 5.550$. At $J_1 = 1.408$, the spin current is larger in the five-membered ring compared with that in the seven-membered ring. Also, the direction of spin currents is opposite in the two rings. The spin currents are also not uniform for all the bonds, implying the mean angle between the spins depends on the bond, as the spin current of a bond is a measure of the angle between orientations of the spins of the bond. The rung bonds have smaller currents than the leg bonds and in the five-membered ring, the upper leg has larger currents than the lower leg, while it is the opposite in the seven-membered ring. The spin current in the five-membered ring almost vanishes at $J_1 = 5.550$, while it is much weaker in the seven-membered ring. The spin currents of the rung bonds are very small and the spin current on the leg bonds in the seven-membered ring becomes uniform. There is also weak dependence of the spin current on the S^z value of the state for which it is calculated.

TABLE I. Two lowest energy levels from different S^z sectors at specified J_1 values (see Fig. 6).

J_1	$E(S^z = 0)$	$E(S^z = 1)$	$E(S^z = 2)$	$E(S^z = 3)$	$E(S^z = 4)$
1.07	-23.8471 -23.8470	-23.8470			
1.408	-25.0575 -25.0574	-25.0575 -25.0574	-25.0574		
4.601	-44.7871 -44.7871	-44.7871 -44.7871	-44.7871 -44.7871	-44.7871	
5.55	-51.7948 -51.7946	-51.7948 -51.7946	-51.7948 -51.7946	-51.7948 -51.7946	-51.7946

TABLE II. Spin currents for different J_1 values in different S^z sectors. At $J_1 = 1.07$, $S = 0$ and $S = 1$ are degenerate. At $J_1 = 1.408$, $S = 1$ and $S = 2$ are degenerate. At $J_1 = 4.601$, $S = 2$ and $S = 3$ are degenerate, and finally at $J_1 = 5.5$, $S = 4$ and $S = 5$ are degenerate; κ_z is defined in Eq. (4).

J_1	S^z	$\kappa_z(1, 2)$	$\kappa_z(4, 5)$	$\kappa_z(1, 3)$	$\kappa_z(5, 7)$	$\kappa_z(2, 4)$	$\kappa_z(4, 6)$
1.07	0	-0.302	-0.302	0.165	-0.158	-0.237	0.086
1.408	0	-0.316	-0.316	0.225	-0.220	-0.315	0.129
	1	0.274	0.274	-0.195	0.190	0.273	-0.112
4.601	0	-0.045	0.045	0	0.205	0	-0.205
	1	-0.042	0.042	0	0.193	0	-0.193
	2	0.033	-0.033	0	-0.153	0	0.153
5.55	0	0.027	-0.027	0	-0.147	0	0.147
	1	-0.026	0.026	0	0.143	0	-0.143
	2	-0.023	0.023	0	0.127	0	-0.127
	3	-0.018	0.018	0	0.097	0	-0.097

IV. SUMMARY AND CONCLUSION

In this paper, we study quantum phases of a spin-1 HAF model on a 5/7 ladder shown in Fig. 1(b). This system goes from a nonmagnetic state to a partially magnetized state for $J_1 > 1.06$, and for $J_1 > 1.44$, magnetization per unit cell is $m = S_G/n = 1$. The gs again goes to a nonmagnetic state for $4.74 < J_1 < 5.44$, and spins have noncollinear arrangement in this phase. For large $J_1 > 5.63$, the gs goes to a magnetic state with $m = 2$.

The correlation length in the 5/7 ladder decreases monotonically with J_1 and for $J_1 = 1$ the correlation length $\xi \sim 3$ lattice units in the singlet gs. The bond order of the rung bonds increase monotonically with J_1 , and in the large J_1 limit, the gs is a product of rung dimers and free spins at 3 and 7 sites in each unit cell. The uniform VBS state of spin-1 chain disappears even for the small value of J_1 as spin-1/2 at the edges of the ladder gets pinned by the rung interaction and forms singlet pairs. In large J_1 limit, the spins at sites $8i - 2$ and $8i$ (i is the unit cell index) form a strong singlet dimer, which is comparable to a spin-1 singlet dimer with bond order ~ 2.0 . Thus, in the large J_1 limit we have a VB state with singlets on the rung bonds and between sites 6 and 8 in each unit cell. The free spins at sites $8i + 3$ and $8i + 7$ have ferromagnetic alignment.

For $J_1 < 1.06$, Γ_σ vanishes and reflection symmetry is broken leading to dimer order in the system. For larger J_1 values, the gs is in a ferrimagnetic state and for some J_1 values the lowest energy states in the even-even and odd-odd subspace under reflection and spin inversion become degenerate. This leads to both inversion and spin-parity symmetry being broken at the degeneracy points; therefore, the gs at this J_1 value possesses vector chirality and there is spontaneous spin current in the ladder system. This is unique as it can have

both finite magnetization and spin current in the absence of an external magnetic field. In this system, maximum gs magnetization per unit cell, $m = 2$, while for a spin-1/2 system, $m = 1$ [43,45]. In the spin-1/2 system magnetic moments are localized mostly on $(4i - 1)$ sites of the system and other sites have vanishingly small spin density [43,45]. However, in the spin-1 system while magnetization contribution comes mostly from sites $(4i - 1)$, there is antiferromagnetically aligned spin density in the lower leg and ferromagnetically aligned spins in the upper leg due to strong singlet dimer formation along the rung. The isolated singlet spin-1 dimer between sites $8i - 2$ and $8i$ in this extended system is unique.

In conclusion, the HAF spin-1 system on a skewed 5/7 ladder is unique with different ferrimagnetic gs, and this system exhibits a plethora of exotic phases in the gs on tuning J_1 . The spin arrangements of the spin-1 system are vastly different from those on the spin-1/2 on this lattice. This is a unique ladder system where a singlet spin-1 dimer and a BOW can coexist. The topological phase of the spin-1 chain vanishes for any finite value of J_1 . The HAF 5/7 ladder system can be mapped onto a spin-1 chain with an AF nearest- and next-nearest-neighbor interaction J_1 and J_2 with periodically missing J_1 bonds. This system may be realized in molecular magnets based on transition metal compounds.

ACKNOWLEDGMENTS

M.K. thanks the Department of Science and Technology (DST), India for Ramanujan fellowship. S.R. thanks the Indian National Science Academy and DST-Science and Engineering Research Board for supporting this work.

S.D. and D.D. contributed equally to this work.

- [1] C. K. Majumdar and D. K. Ghosh, *J. Math. Phys.* **10**, 1388 (1969); **10**, 1399 (1969).
 [2] T. Hamada, J.-i. Kane, S.-i. Nakagawa, and Y. Natsume, *J. Phys. Soc. Jpn.* **57**, 1891 (1988).
 [3] A. V. Chubukov, *Phys. Rev. B* **44**, 4693 (1991).

- [4] R. Chitra, S. Pati, H. R. Krishnamurthy, D. Sen, and S. Ramasesha, *Phys. Rev. B* **52**, 6581 (1995).
 [5] S. R. White and I. Affleck, *Phys. Rev. B* **54**, 9862 (1996).
 [6] C. Itoi and S. Qin, *Phys. Rev. B* **63**, 224423 (2001).
 [7] S. Mahdavi, *J. Phys.: Condens. Matter* **20**, 335230 (2008).

- [8] J. Sirker, *Phys. Rev. B* **81**, 014419 (2010).
- [9] M. Kumar, A. Parvej, and Z. G. Soos, *J. Phys.: Condens. Matter* **27**, 316001 (2015).
- [10] Z. G. Soos, A. Parvej, and M. Kumar, *J. Phys.: Condens. Matter* **28**, 175603 (2016).
- [11] M. Kumar, S. Ramasesha, and Z. G. Soos, *Phys. Rev. B* **81**, 054413 (2010).
- [12] M. Kumar and Z. G. Soos, *Phys. Rev. B* **85**, 144415 (2012).
- [13] T. Vekua, A. Honecker, H.-J. Mikeska, and F. Heidrich-Meisner, *Phys. Rev. B* **76**, 174420 (2007).
- [14] T. Hikihara, L. Kecke, T. Momoi, and A. Furusaki, *Phys. Rev. B* **78**, 144404 (2008).
- [15] J. Sudan, A. Läuscher, and A. M. Läuchli, *Phys. Rev. B* **80**, 140402(R) (2009).
- [16] D. V. Dmitriev and V. Y. Krivnov, *Phys. Rev. B* **77**, 024401 (2008).
- [17] F. Heidrich-Meisner, A. Honecker, and T. Vekua, *Phys. Rev. B* **74**, 020403(R) (2006).
- [18] F. Heidrich-Meisner, I. A. Sergienko, A. E. Feiguin, and E. R. Dagotto, *Phys. Rev. B* **75**, 064413 (2007).
- [19] F. Heidrich-Meisner, I. P. McCulloch, and A. K. Kolezhuk, *Phys. Rev. B* **80**, 144417 (2009).
- [20] A. Parvej and M. Kumar, *Phys. Rev. B* **96**, 054413 (2017).
- [21] L. Kecke, T. Momoi, and A. Furusaki, *Phys. Rev. B* **76**, 060407(R) (2007).
- [22] F. D. M. Haldane, *Phys. Lett. A* **93**, 464 (1983); *Phys. Rev. Lett.* **50**, 1153 (1983).
- [23] I. Affleck, T. Kennedy, E. H. Lieb, and H. Tasaki, *Phys. Rev. Lett.* **59**, 799 (1987).
- [24] I. Affleck, T. Kennedy, E. H. Lieb, and H. Tasaki, *Commun. Math. Phys.* **115**, 477 (1988).
- [25] U. Schollwöck, O. Golinelli, and T. Jolicœur, *Phys. Rev. B* **54**, 4038 (1996).
- [26] S. Östlund and S. Rommer, *Phys. Rev. Lett.* **75**, 3537 (1995).
- [27] F. Verstraete, V. Murg, and J. Cirac, *Adv. Phys.* **57**, 143 (2008).
- [28] U. Schollwöck, *Ann. Phys.* **326**, 96 (2011).
- [29] S. R. White, *Phys. Rev. Lett.* **69**, 2863 (1992).
- [30] S. R. White, *Phys. Rev. B* **48**, 10345 (1993).
- [31] U. Schollwöck, *Rev. Mod. Phys.* **77**, 259 (2005).
- [32] K. A. Hallberg, *Adv. Phys.* **55**, 477 (2006).
- [33] R. Orús, *Ann. Phys.* **349**, 117 (2014).
- [34] F. Verstraete and J. I. Cirac, *Phys. Rev. A* **70**, 060302(R) (2004).
- [35] T.-C. Wei, I. Affleck, and R. Raussendorf, *Phys. Rev. Lett.* **106**, 070501 (2011).
- [36] M. Lemm, A. W. Sandvik, and L. Wang, *Phys. Rev. Lett.* **124**, 177204 (2020).
- [37] N. Pomata and T.-C. Wei, *Phys. Rev. Lett.* **124**, 177203 (2020).
- [38] D. Dey, M. Kumar, and Z. G. Soos, *Phys. Rev. B* **94**, 144417 (2016).
- [39] S. R. White and D. A. Huse, *Phys. Rev. B* **48**, 3844 (1993).
- [40] S. Todo, M. Matsumoto, C. Yasuda, and H. Takayama, *Phys. Rev. B* **64**, 224412 (2001).
- [41] T. Hikihara, M. Kaburagi, and H. Kawamura, *Prog. Theor. Phys., Suppl.* **145**, 58 (2002).
- [42] N. Chepiga, I. Affleck, and F. Mila, *Phys. Rev. B* **93**, 241108(R) (2016).
- [43] G. Giri, D. Dey, M. Kumar, S. Ramasesha, and Z. G. Soos, *Phys. Rev. B* **95**, 224408 (2017).
- [44] S. Thomas, S. Ramasesha, K. Hallberg, and D. Garcia, *Phys. Rev. B* **86**, 180403(R) (2012).
- [45] D. Dey, S. Das, M. Kumar, and S. Ramasesha, *Phys. Rev. B* **101**, 195110 (2020).